

Annex 1

Gas circulation / purification system

In the proposed experiment, a high pressure hydrogen TPC and a large aperture Forward Tracker are placed in one vessel which could stand for pressures up to 25 bar (Fig.1) These detectors operate with different gas fillings: ultra-clean hydrogen in TPC and Ar+1%CH₄ in the tracker. The main body of the detector is made of normal steel which is not clean enough for the purposes of this experiment. Therefore, TPC and PC have individual clean volumes (made of stainless steel with thin beryllium and capton windows) surrounded by technical Argon (Fig.1). So, there are three different gas volumes where the pressure should be permanently equalized. Also, this pressure should be stable, and its value should be known with 0.01% absolute precision. The measurements will be performed at 20 bar and at 4 bar gas pressure. In order to avoid the losses of the ionization electrons during the drift time, the contamination of the H₂ gas by any electro-negative gas (O₂, H₂O) should be reduced to a level below 1 ppm. This will be achieved by continuous H₂ purification with a special cryogenic gas purification system which eliminates gas impurities down to ~ 0.1 ppm.

The system satisfying the above formulated requirements has been designed at PNPI. This design is based on the experience from operation of a hydrogen gas circulation/purification system previously constructed for the MuCap experiment at PSI [1].

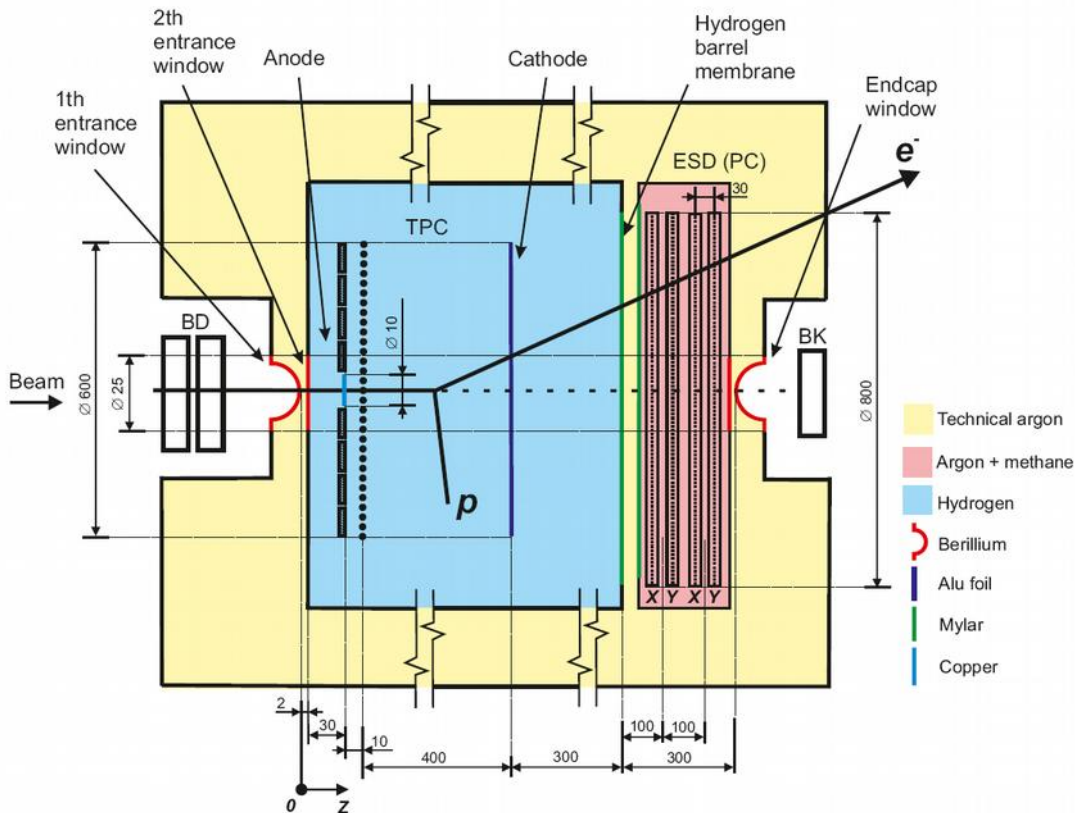


Fig. 1. Schematic view of the TPC & FT detector with three gas volumes (H₂, Ar+1%CH₄, and Ar) in a common high pressure vessel.

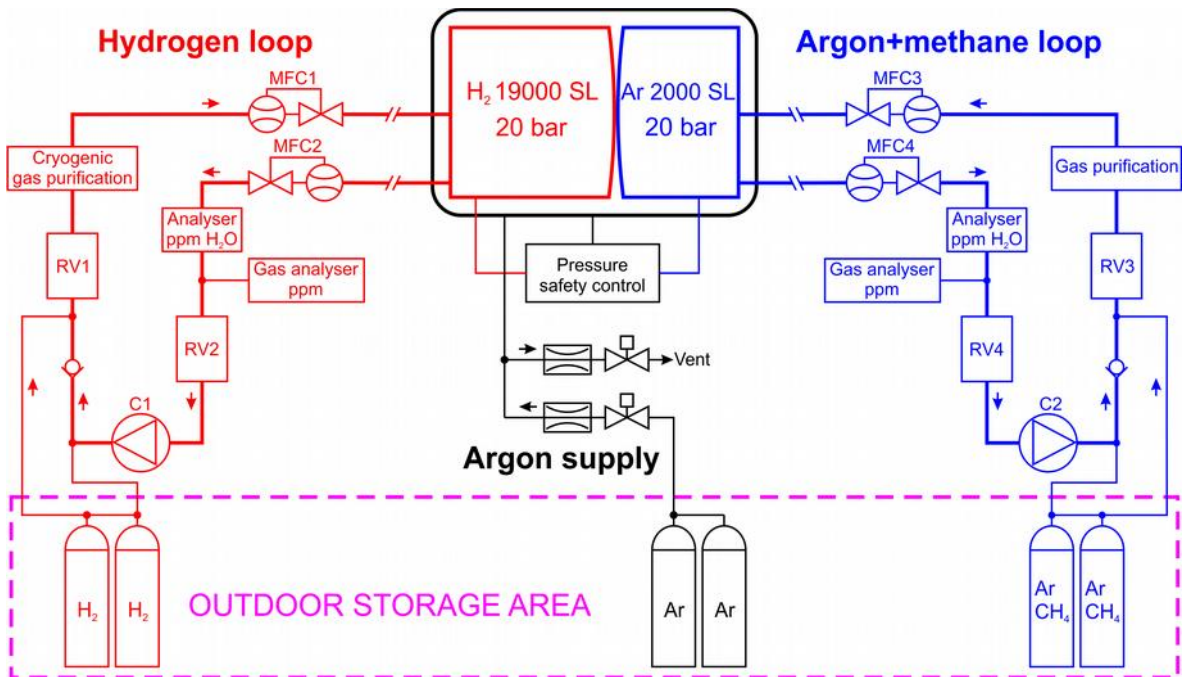


Fig. 2. Simplified diagram of the gas circulation/purification system.

Fig.2 shows a simplified diagram of the gas system designed for this experiment. Fig.3 presents the complete technical design of this system. It consists of three independent subsystems.

1. The hydrogen subsystem for TPC, volume about 1 cubic meter. The gas circulation is maintained by compressor C1. This subsystem:
 - Purifies hydrogen in TPC down to < 1 ppm impurities level with a gas flow of 15 normal liters per minute;
 - Stabilizes hydrogen pressure in the detector with stability 2 mbar in the range 4-20 bar with the help of mass-flow controllers MFC1 and MFC2 and reserve volumes RV1 and RV2 suppressing the pressure oscillations before and after compressor C1;
 - Gives possibility to analyze the gas purity in TPC on a sub ppm level using a “water analyzer” and an oxygen analyzer;
 - Evacuates hydrogen into the hydrogen reserve volume with typical filling/evacuation time of 20-40 hours.
2. The Argon+methane subsystem for the Forward Tracker operating in the same way as the hydrogen subsystem. The gas purification is adopted for the argon+methane gas mixture and includes periodically replacing of some fraction of the gas mixture by a fresh gas mixture.
3. The Argon supply subsystem does not use gas circulation. The pressure in this subsystem is regulated by adding and venting argon via electromagnetic valves. This pressure is equalized with the pressure in TPC@FT during all operations with the gases (circulation, filling and evacuation of hydrogen and argon+methane gas mixture).

Slow control system provides minimization (1-2 mbar) of the differential pressure between all subsystems during normal gas circulation and during filling-evacuation procedure.

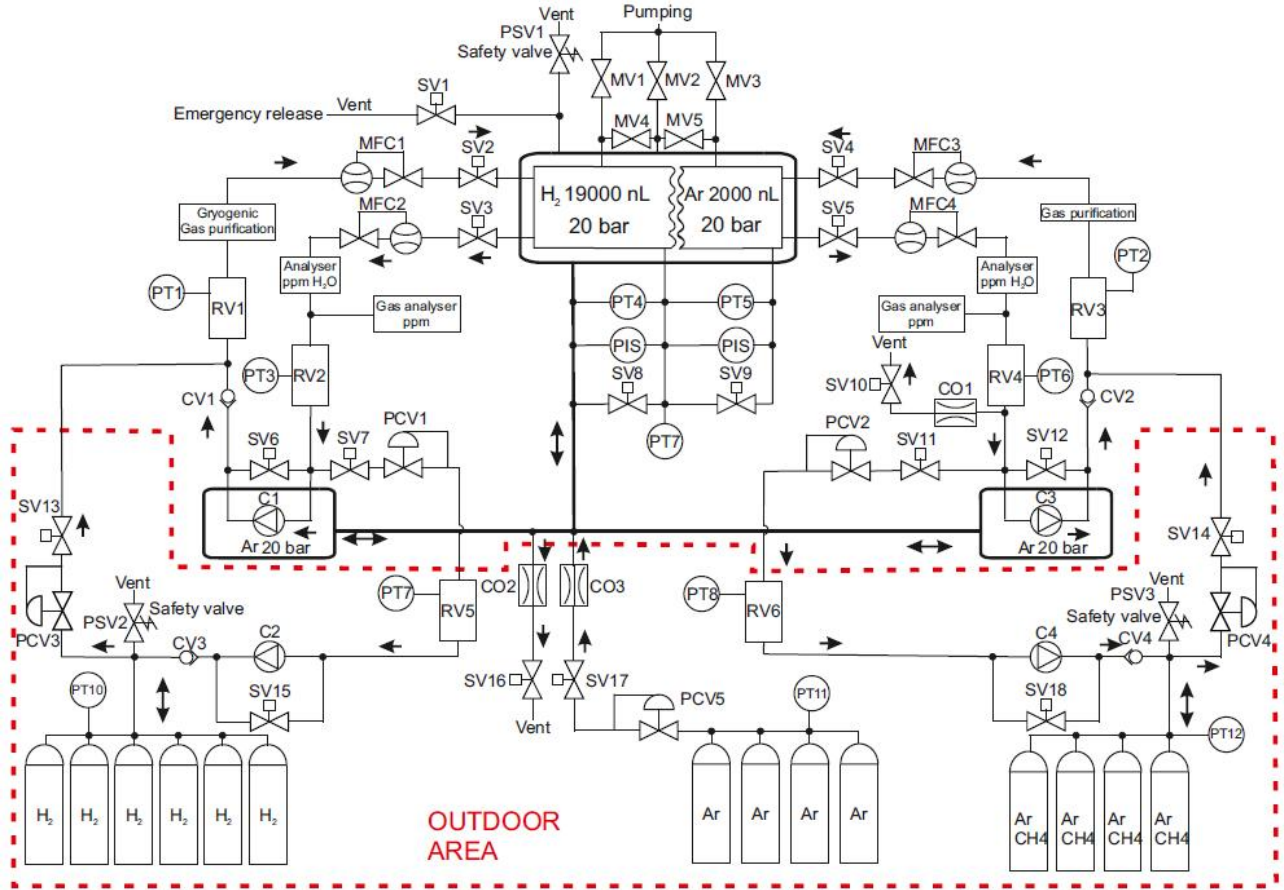


Fig. 3. Complete technical design of the gas circulation/purification system

MV – manual valve

SV – remotely operated valve

PT – pressure transmitter (sensor) for absolute and differential pressure measurements

MFC – mass-flow controller

PSV – release safety valve

RV – reserve volume

PCV – reduction valve

CV – check valve

PIS – pressure indicator

CO – capillary throttle

C - compressor

Reference

1. A circulating hydrogen ultra-high purification system for the MuCap experiment. V.A. Andreev et al. NIM A578 (2007) 485.

Annex 2

Test run with a TPC prototype

A2 hall, 720 MeV electron beam, August-September 2017

The main goal of the test run was to investigate performance of the TPC in the electron beam. In particular, one had to answer the following questions:

- How much the recoil proton energy resolution is deteriorated in presence of the electron beam with intensity up to 2 MHz?
- What is the background in TPC and occupancy of the read out channels? Would it be possible to operate TPC in the self-triggering mode?

Also, it was important to obtain the electron beam with requested parameters: strongly reduced intensity (2 MHz, 100 kHz, 10 kHz), ≤ 0.5 mrad (sigma) divergence, ≤ 0.5 mm (sigma) size, stable beam spot position and intensity. In addition, the pixel detectors were to be tested for control of the beam size and position.

The experimental setup used in this test run was a TPC constructed within the program FAIR at GSI as an ACTAR2 prototype of the Active Target for the R3B experiment. Previously, it has been used in a test experiment at GSI with 700 MeV/u heavy ions beams. This TPC is similar to the TPC in our proposal (though smaller in size and with lower pressure), and it could help to answer the formulated above questions. Normally, this TPC operates with hydrogen gas filling up to 10 bar pressure, but it was filled with the gas mixture of He+4%N₂ in this run because of safety restrictions to work with hydrogen at this stage of construction of the experimental setup. However, as it was shown by our MC simulation, the ionization properties of this gas mixture are similar to those in hydrogen. Therefore, the obtained results could be used for predictions for the hydrogen TPC performance designed for the main experiment.

A schematic view of the layout of the ACTAR2 prototype is shown in Fig 1. The system of the TPC electrodes – the cathode, the grid, and the sectioned plane of anodes is placed inside a 40 liters cylindrical aluminum vessel. The semi-spherical beam windows of beryllium, 0.5 mm thick, 70 mm in diameter are mounted on the forward and backward flanges of the vessel.

The anode-grid distance is 3 mm, the grid-cathode distance (the drift gap) is 220 mm. The field uniformity in the drift gap is formed by a set of 11 field shaping rings. The grid is made of 55 μ m steel wires wound with 1 mm step on a stainless steel ring (204 mm internal diameter). The anode outer diameter is 200 mm. The anode electrode is split into 66 segments (Fig. 2). The measurements were performed with 10 bar and 5 bar gas pressure. The potentials on the cathode and on the grid, as well as the corresponding drift velocities are shown in Table 1. The anode is at zero potential.

Table1 ACTAR2 prototype operational conditions in the test run.

| Gas pressure | HV cathode | HV grid | Drift velocity Cathode-grid | Drift velocity Grid-anode |
|--------------|------------|---------|-----------------------------|---------------------------|
| 10 bar | - 14 kV | - 0.8 | 2.75 mm/ μ s | 6 mm/ μ s |
| 5 bar | - 9 kV | -0.5 | 3.14 mm/ μ s | 9 mm/ μ s |

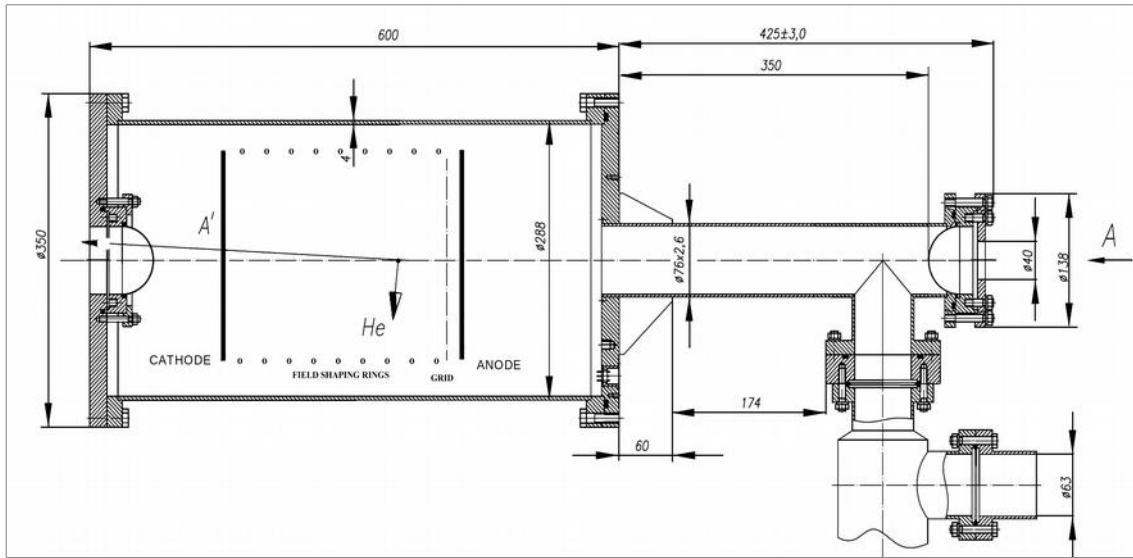


Fig. 1. Schematic view of the ACTAR2 prototype (side view).

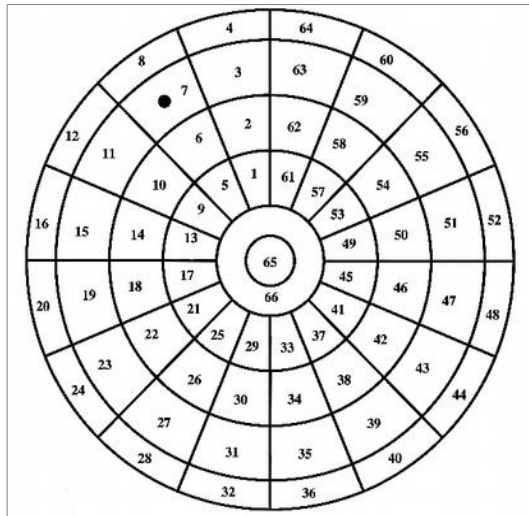


Fig. 2. Layout of the ACTAR2 prototype anodes. An ^{241}Am α -source is deposited on the cathode of the chamber opposite to the black spot on the anode number 7. The outer diameter of the anode plane is 200 mm. The central pad is 20 mm in diameter.

Signals from all anodes are read out by independent electronics channels including preamplifiers, amplifiers, and Flash-ADCs (14 bit, 250 MHz). The signal shaping was

optimised to get maximal signal-to-noise ratio. The resulted energy resolution was around 20 keV in all anode channels. Fig. 3 illustrates the shaping of the signals in the amplifiers (reaction on a delta function input signal)

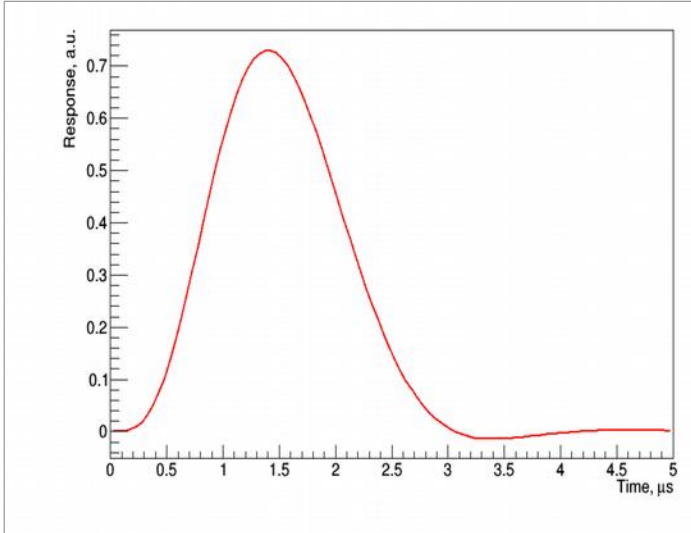


Fig. 3. Signal at the output of the amplifier corresponding to a delta function input signal.

The beam tracking detectors were placed upstream of the TPC. These were 4 planes of $3 \times 3 \text{ mm}^2$ pixel detectors (0.05 mm thickness, $100 \times 80 \text{ μm}^2$ pixels). In addition, there were one scintillator upstream and one scintillator downstream of TPC. The experimental setup was implemented in the GIANT4 MC model (Fig.4)

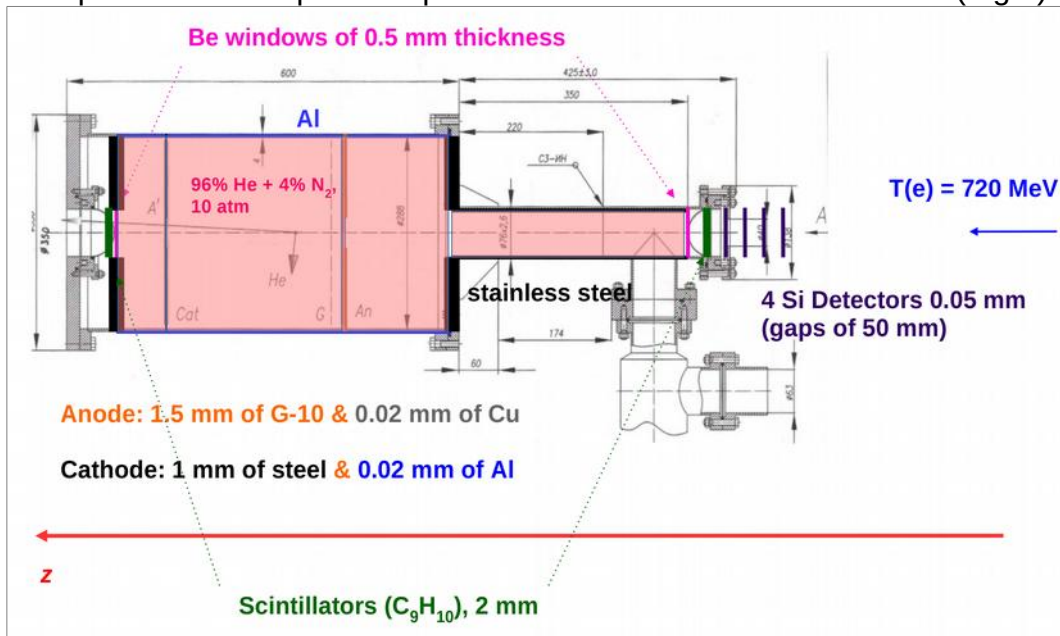


Fig. 4. The experimental setup as implemented in the GIANT4 Monte Carlo model.

The experimental setup was installed in A2 hall downstream of the Cristal Ball/Taps setup. (Fig.5). A temporary electron beam line was constructed specially for this

experiment. The beam was focused on the input of the ACTAR2 setup. The parameters of the beam were measured with the pixel detectors (Fig.6). According to these measurements, the size of the beam spot was $250\ \mu\text{m}$ (sigma), and divergence was 1mrad, which is close to the requirements of the experiment. Critical for this experiment was stability of the electron beam at unusually for MAMI low beam intensity (2MHz, 100 kHz, and 10 kHz). All these options were successfully tested in the run.

It was demonstrated that MAMI can provide practically ideal electron beams for this experiment. The only concern was some long term instability of the beam spot. Therefore, it should be under control in the main experiment with feed back to the accelerator control room.



Fig.5. Plan of A2 hall. The ACTAR2 setup is installed downstream of the Cristal Ball/Taps setup. A temporary electron beam line was constructed for this test run. Also shown is a new electron beam line designed especially for this experiment.

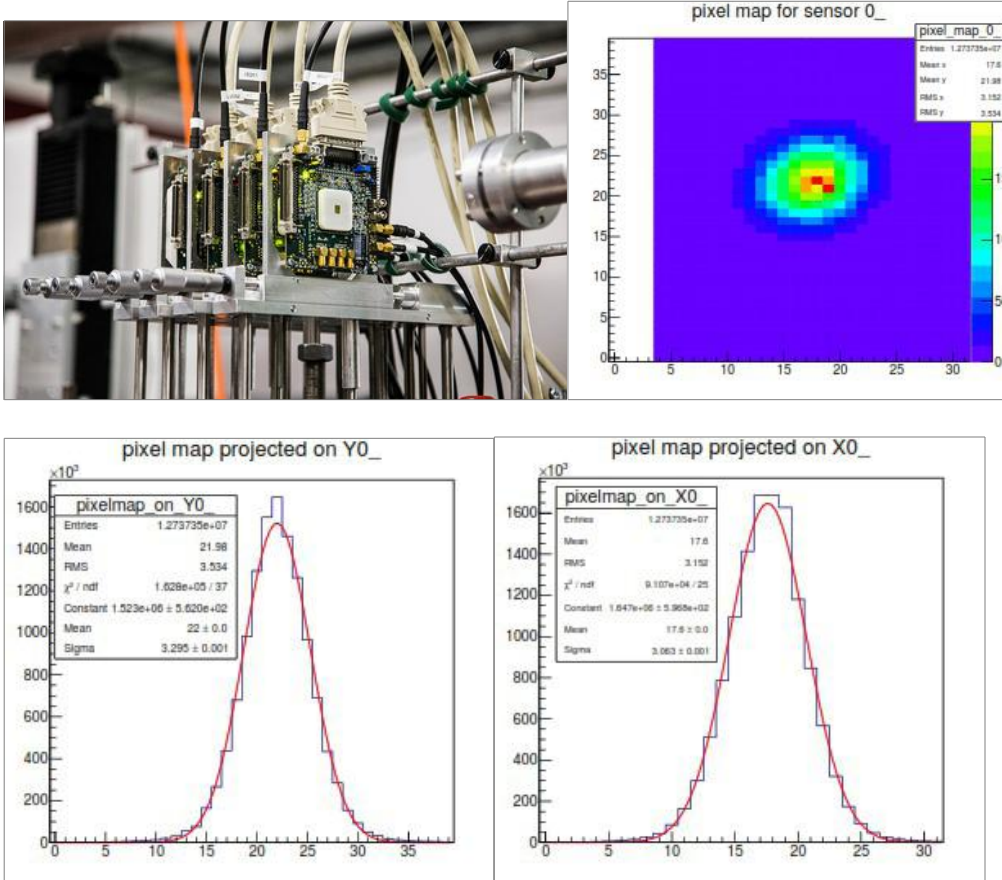


Fig. 6. Beam telescope - four planes of pixels (top left). Beam spot as seen by pixels (top right). Pixel map projections in Y0 (bottom left) and X0 (bottom right) planes. The x-axis in the figure is the pixel numbers. (the pixel width is 80 μm and 100 μm for Y0 and X0 planes, respectively).

Recoil energy resolution

Every beam particle produces ionization in TPC along its track with fluctuations caused mostly by emission and absorption of delta electrons. With the total drift time 100 μs and the beam intensity 2 MHz, the ionization produced by ~ 200 particles remains permanently in the TPC volume. This results in the “beam ionization noise” in addition to the electronics noise. Such processes are included in the GIANT4 MC model. With this model, the expected beam ionization noise was calculated for the ACTAR2 TPC.

Fig.7 shows the simulated 1.5 MeV recoil signals at the central anode channel mixed with the beam ionization noise at 1.5 MHz and 0.7 MHz beam rates. The measured width of the signal amplitude distribution gives the “beam ionization noise”. To obtain the total noise, one should add the electronics noise which is 20 keV (sigma) in our case.

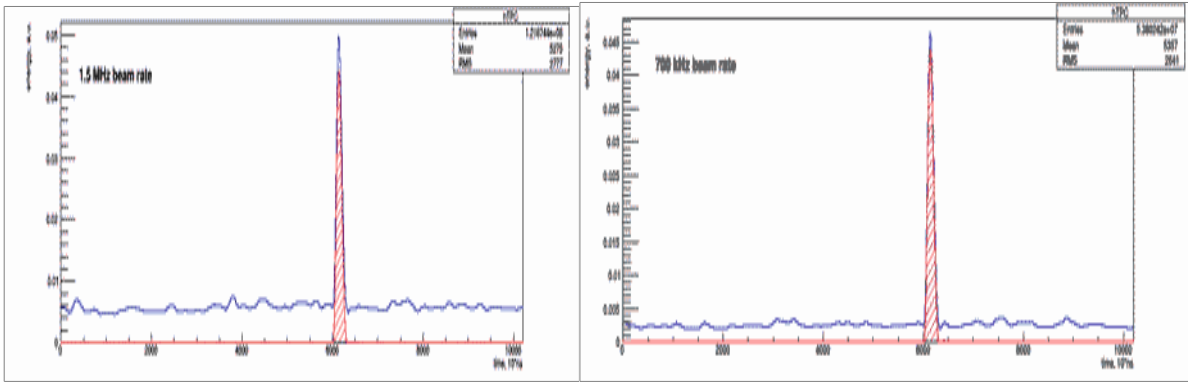


Fig.7. Simulated 1.5 MeV signals on top of the “beam ionization noise” for 1.5 MHz (left) and 0.7 MHz (right) beam rates.

The MC simulation was performed for various beam rates and experimental conditions. The obtained results are presented in Fig.8 a,b,c.

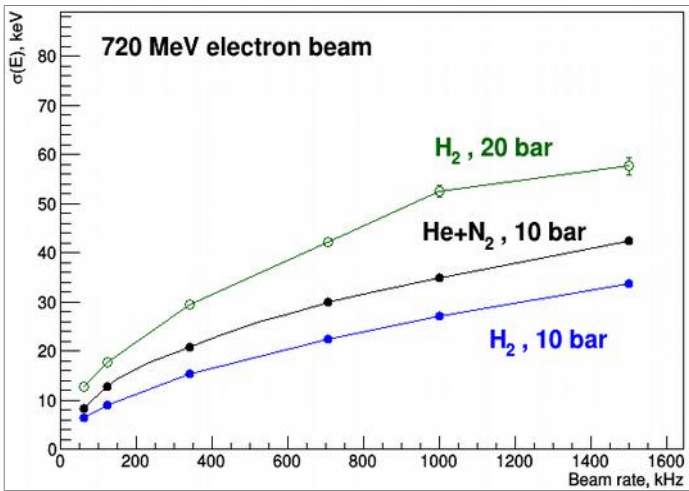


Fig.8a. Beam ionization noise in function on the beam rate calculated for the He + 4%N₂ gas mixture (10 bar) and for pure hydrogen (10 bar and 20 bar). Drift gap 220 mm. Drift velocity 2.75 mm/μs.

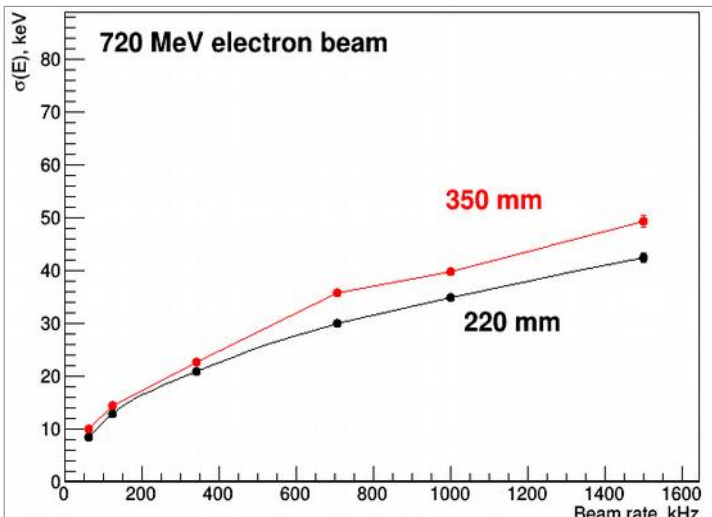


Fig.8b. Beam ionization noise in function on the beam rate calculated for drift gaps 220 mm and 350 mm He + 4%N₂ gas mixture (10 bar). Drift velocity 2.75 mm/μs.

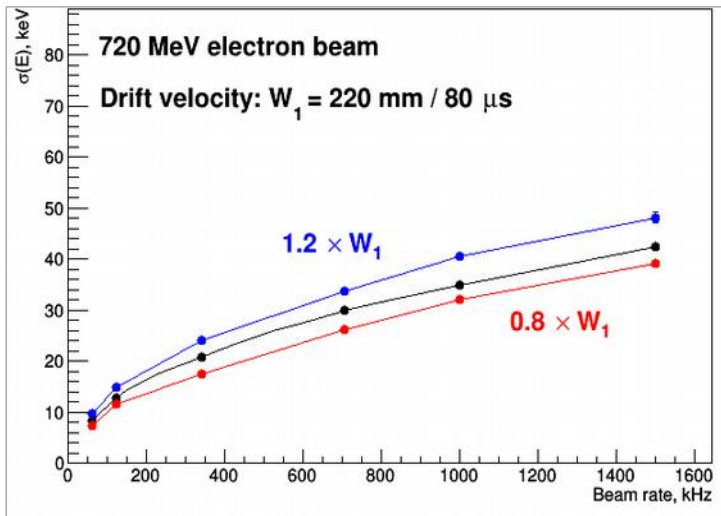


Fig.8c. Beam ionization noise in function on the beam rate calculated for various drift velocities. He + 4%N₂ gas mixture (10 bar). drift gap 220 mm.

The results of the MC simulations could be summarized as follows:

- The beam noise is increasing with beam rate as root square of the rate;
- The beam noise is nearly proportional to the gas pressure;
- The beam noise is increasing slightly with the total drift gap;
- The beam noise is increasing slightly with the drift velocity;
- The beam noise in hydrogen is less than in the He+4%N₂ mixture by ~ 20%.

The measurements of the noise in the test run have been done with pulse generator signals sent simultaneously to the inputs of all anode channels. The extraction of the signals and determination of the width was done with the same algorithm as in the MC studies. The measurements were performed at 10 bar and 5 bar gas pressure at various beam rates. **These measurements showed that the beam noise appears mostly in the central anode pad № 65 and too much less extent on the nearest ring (pad № 66).** The noise on all other pads is practically insensitive to the beam rate. The results of the noise measurements on the central pad are presented in Fig.9 together with the MC results.

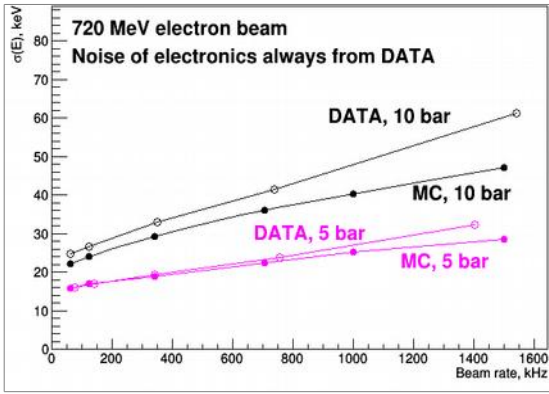


Fig.9. Comparison of the noise at the central pad measured at various beam rates with MC calculations. He + 4%N₂ gas mixture (5 bar and 10 bar). Drift gap 220 mm. Drift velocity 2.75 mm/μs for 10 bar and 3.14 mm/μs for 5 bar gas pressure. Note that the calculated beam ionization noise was summed up with the electronics noise in this figure for comparison with the experimental data.

One can see that the experimental results are in reasonable agreement with the Monte Carlo calculations. Based on this agreement, we can use the MC model for prediction of the beam noise conditions in our main experiment. The results are presented in Fig. 10.

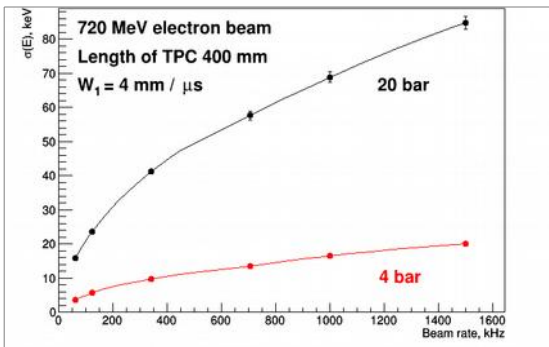


Fig.10. MC prediction of the beam ionization noise on the central pad for the main experiment. Pure hydrogen. 20 bar and 4 bar gas pressure. Drift gap 400 mm. Drift velocity 4 mm/μs.

According to these calculations,

The expected noise on the central pad in the main experiment is ~ 90 keV at 20 bar and ~ 30 keV at 4 bar hydrogen gas pressure.

TPC rates in self-triggering mode

The rates of the self-triggers were measured with the following definition of the trigger signal. The thresholds in each anode channel were set at 300 keV. The trigger was generated when there was at least one signal exceeding this threshold. After that, the information was read out from all anode channels. Note that the energy scale was calibrated by the position of the ²⁴¹Am alpha peak in the ADC channels.

The following results have been obtained at 1.6 MHz (10 bar pressure):

| | |
|--|--------|
| Total rate of self-triggers | 8 Hz |
| Signals from the central pad with no signals from other pads | 5.6 Hz |
| Signals from the central pad in coincidence with any other pad | 0.6 Hz |

The observed number of self-triggers includes also the real $e^4\text{He}$ elastic scattering as well as the inelastic reactions on ^4He and Nitrogen. An example of such events is presented in Fig.11 showing a long range track started from the central pad.

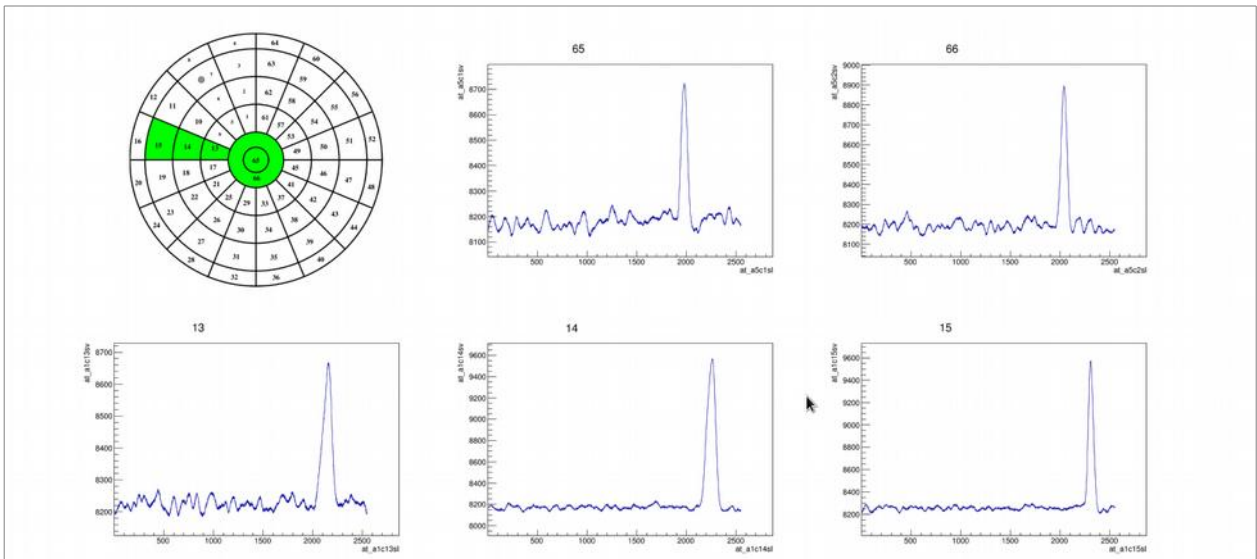


Fig.11. Display of a long range track observed in the TPC.

The calculated rate of the $e^4\text{He}$ elastic scattering events in the covered Q^2 range (recoil ^4He energy ≥ 300 keV) is 3.5Hz, the majority of these events being within the central pad. That means that **the observed self-trigger rate is determined mostly by the physics reactions with only little contribution from the beam ionization noise.** This statement is supported by direct measurement of the amplitude spectrum of the signals from the central pad (Fig.12).

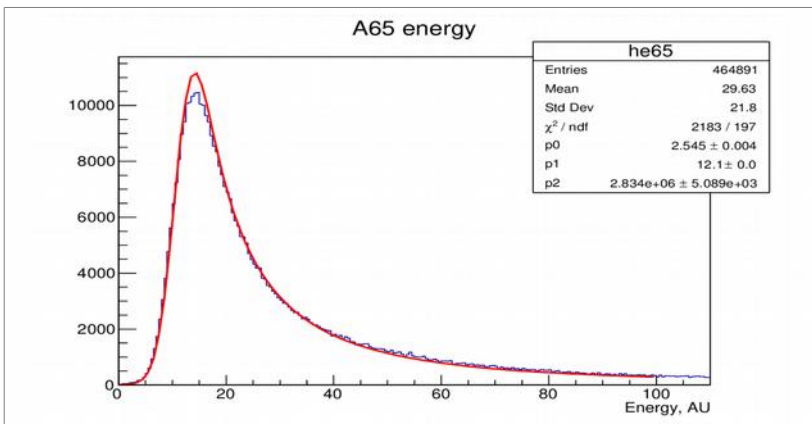


Fig. 12. Amplitude distribution of the signals from the central pad. Scale is in the ADC channels, 1 ch=22 keV. The red curve – fit with $1/t^2$ distribution combined with a Gaussian centered at 300 keV.

In the main experiment, the self-trigger rate will be determined by the rate of the ep-elastic cross section in the selected Q^2 range. With the beam rate 2 MHz and the threshold at 300 keV, it will be ~ 30 Hz at 20 bar and ~ 6 Hz and 4 bar hydrogen gas pressure. Note that the threshold at the central pad should be probably increased in the 20 bar runs up to ~ 450 keV due to higher beam ionization noise (five $\sigma_{\text{noise}} \sim 90$ keV) that will reduce the trigger rate to ~ 20 Hz. Anyhow, we can formulate a very important conclusion for planning the read out system in the main experiment:

For triggering, one can use the self-trigger from TPC with the mean rates ≤ 50 Hz.

Conclusions from the test run

- MAMI accelerator provides practically an ideal electron beam for this experiment.
- The beam ionization noise produced in TPC by the electron beam is in agreement with the Monte Carlo simulations. No unexpected sources of the background in TPC has been manifested. This allowed to make predictions for the noise and background conditions in the main experiment.
- For triggering, one can use the self-trigger from TPC with the mean rates ≤ 50 Hz.

The above conclusions have been drawn from measurements with TPC filled with the 4He +4%N₂ gas mixture. It would be important to repeat these measurements with hydrogen gas in TPC, resolving for that the safety problems. Another important task for the next test run is testing and calibration of the beam counters which should operate in the 2 MHz beam with minimum dead time to provide high precision information on the absolute beam rate.

Participants in the test run and data analysis

Mainz: Patrik Adlarson, Marco Dehn, Peter Drexler, Andreas Thomas, Frederik Wauters, Vahe Sokhoyan, Achim Denig, Michael Ostrick, Niklaus Berger, Oleksandr Kostikov Maik Biroth, Edoardo Mornacchi, Jurgen Ahrens.

PNPI: Alexey A. Vorobyov, Alexander Vasilyev, Petr Kravtsov, Marat Vznuzdaev, Kuzma Ivshin, Alexander Solovyev, Ivan Solovyev, Alexey Dzyuba, Evgeny Maev, Alexander Inglessi, Gennady Petrov

GSI: Peter Egelhof, Oleg Kiselev

College of William and Mary: Keith Griffioen, Timothy Hayward

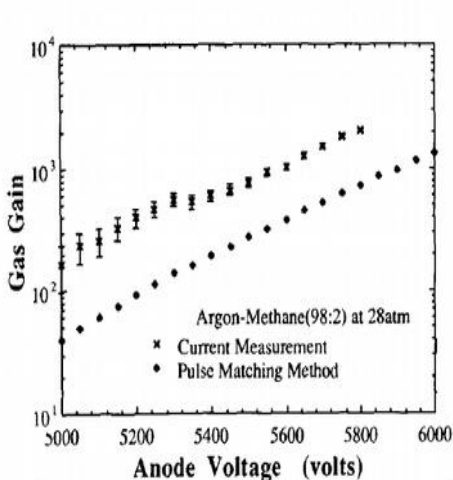
Annex 3

Study of gas gain in a CSC prototype at high pressure

The FT consists of two pairs of Cathode Strip Chambers X_1/Y_1 and X_2/Y_2 . Each chamber is a symmetric MWPC with 2.5 mm gap between the cathode and the anode planes. The size of the chamber is $600 \times 600 \text{ mm}^2$. The readout is from both cathode planes. The anode wire plane contains $30 \mu\text{m}$ wires spaced by 3 mm. Both cathode planes are made with $100 \mu\text{m}$ wires wound with 0.5 mm step. The cathode wires are orthogonal to the anode wires in one cathode plane and inclined by 45 deg. in the other cathode plane. The wires in the inclined cathode plane are grouped into 10 mm strips. In the cathode plane with orthogonal to the anode wires, 2 mm strips are formed by joining together 4 wires. The width of all strips should be identical within $\pm 20 \mu\text{m}$. This allows determination of the center-of gravity of each detected signal with a precision $\sim 1\%$ of the strip width ($\sigma_{\text{proj}} \sim 30 \mu\text{m}$) assuming the signal to noise ratio $S/N \geq 100$ and the electronics amplification uniform within 1% in each readout channel.

The ionization produced in a CSC plane by a relativistic particle is ~ 1000 electrons at 20 bar pressure. The electronics noise is ~ 1000 electrons. Therefore, to obtain the ratio $S/N \geq 100$, the CSC gas gain should be ~ 100 . However, the detected charge is only $\sim 30\%$ of the total charge. Therefore, the gas gain should be at least 300 but better 10^3 . It is not trivial to obtain such gas gain at 20 bar pressure with 600 mm long anode wires. In particular, it is not possible in pure hydrogen. That is why we shall use the Ar + CH₄ gas mixture.

There is very limited information on gas amplification at high gas pressure. To our knowledge, there were only studies of gas gains in a proportional cylindrical counter performed by an Australian group in 1993. They could reach the 10^3 gas gain at 28 bar pressure in the gas mixture Ar + 2% CH₄ (Figure below).



Nuclear Instruments and Methods in Physics Research A329 (1993) 140-150
North-Holland

Gas amplification in high pressure proportional counters

Z. Ye ^a, R.K. Sood ^a, D.P. Sharma ^b, R.K. Manchanda ^c and K.B. Fenton ^b

^a Department of Physics, University College, University of NSW, ADFA, Campbell, ACT 2600, Australia

^b Physics Department, University of Tasmania, Hobart, Tas 7001, Australia

^c Tata Institute of Fundamental Research, Bombay, 400 005, India

Still it was an open question if this result could be reproduced in multiwire proportional chambers. For that purpose, we have performed some tests using a small size prototype of the CSC designed for the Forward Tracker (Fig.1) with the gas mixture Ar+ 1% CH₄.

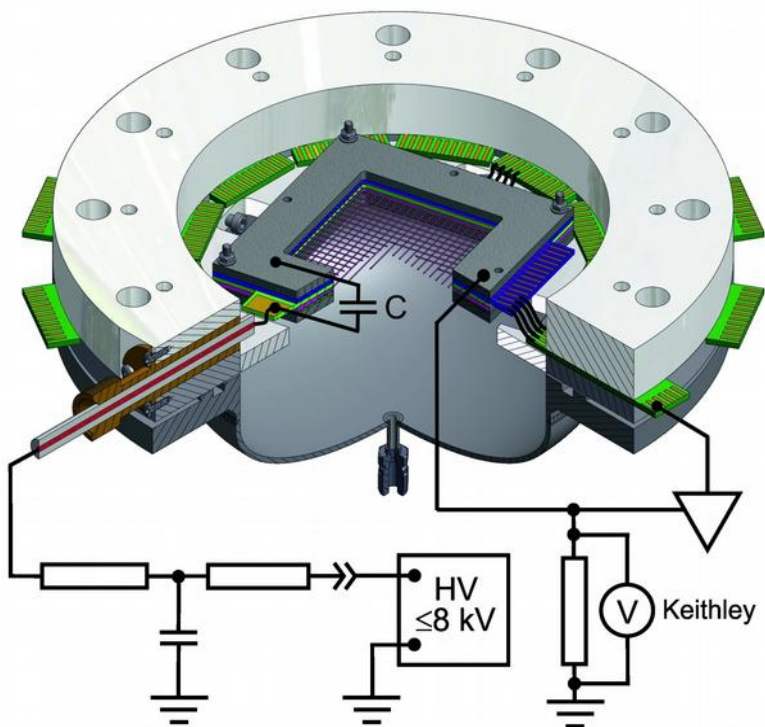


Fig.1. CSC prototype prepared for measuring gas gain at high pressure.

The measurements have been done with a ^{55}Fe x-ray source (6 keV) and also with cosmic muons. Fig. 2 shows the amplitude spectrum measured with the ^{55}Fe x-rays at 20 bar pressure HV= 6100 V. The peak position corresponds to 10^3 gas gain.

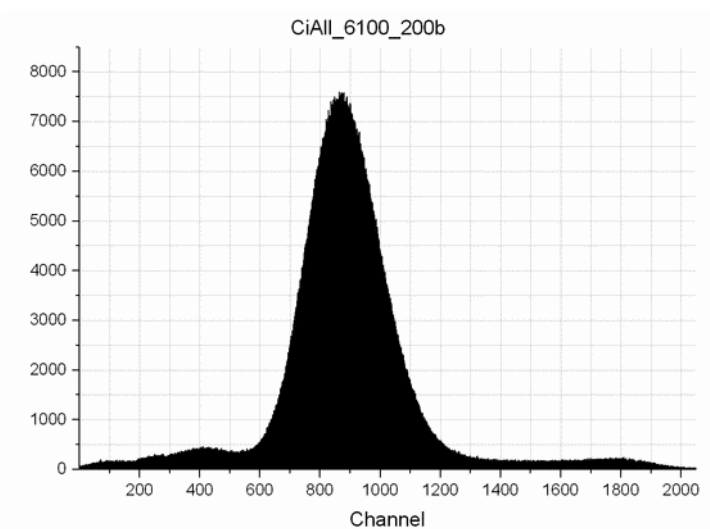


Fig.2. ^{55}Fe source photons amplitude spectrum in 99%Ar+1%CH4 gas mixture at 20 bar. Peak position in 880 ch corresponds to the GG 1000.

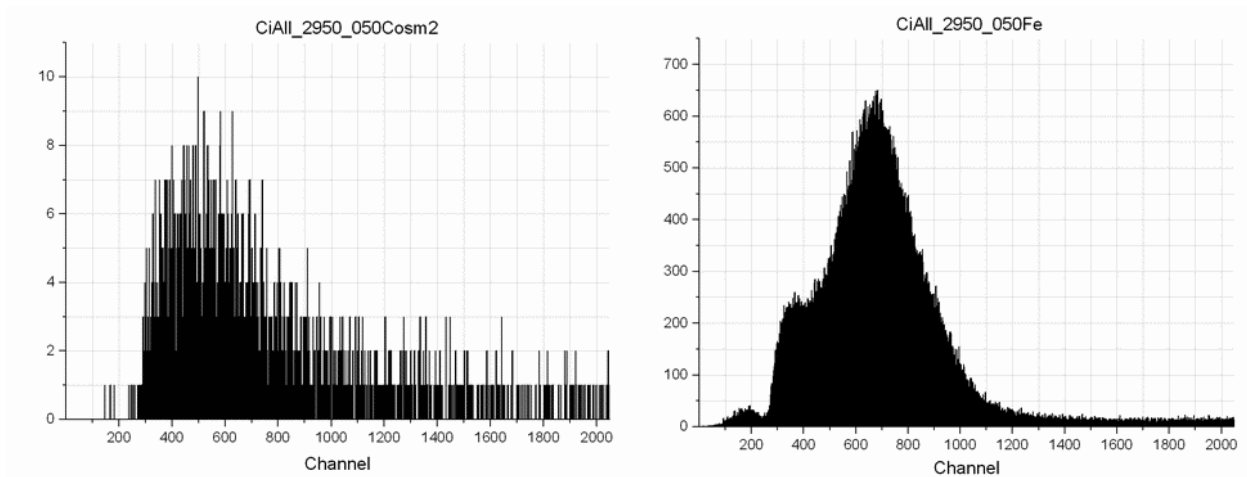


Fig.3. Amplitude spectrum measured with cosmic muons (left) and with ^{55}Fe x-rays (right). $P=5$ bar. $HV=2950V$. $GG =600$ corresponds to channel 700.

Fig.3 shows comparison of the amplitude spectrum measured with the ^{55}Fe x-rays with that measured with cosmic rays at 5 bar pressure. The initial ionizations are comparable for both cases. However, the mean amplitude in the cosmic ray spectrum proved to be by $\sim 20\%$ lower due to different reaction of the amplifier on continuous tracks from muons and short tracks from x-rays.

Conclusions: These tests demonstrated possibility to reach the necessary gas gain $GG=300$ in terms of detected charge at 20 bar pressure.

Annex 4. Trigger, readout, and selection of true ep collisions

Trigger

The choice of the trigger is one of the critical points in the experiment. Fortunately, we have possibility to use the TPC recoil proton signals for triggering the readout system. This is the most safe and effective triggering option.

As it was demonstrated in the test run, the background in TPC produced by the electron beam is rather low. The self-trigger rate from TPC operating at 10 bar pressure was ~ 8 Hz at the beam intensity 1.6 MHz, the trigger being defined as any signal exceeding the 300 keV level in any of 66 anode pads. Most of this rate is due to elastic $e^4\text{He}$ scattering (~ 3.5 Hz) and from inelastic reactions on ^4He and Nitrogen. That means that in the main run with hydrogen in TPC, the self trigger rate would be determined mostly by the ep elastic scattering events. The expected rate of such events is $N_{\text{ep_elastic}} = 30$ Hz with the threshold set at 300 keV at $P=20$ bar and 6 Hz at $P=4$ bar.

Readout

The presented here readout scheme was designed specially for this experiment. The main features of this system:

- Triggering by signals from TPC (self-triggering).
- The maximal average trigger rate: 50 Hz.
- After receiving a trigger signal, the information from all detectors appeared in a regulated time interval (up to 655 μs) before arrival of the trigger is readout from the pipeline and sent to DAQ.
- The number of readout channels: 24 channels from TPC and 1920 channels from Forward Tracker.
- The readout system provides continuous data flow without dead time.

This readout scheme is based on some previous developments at the PNPI Electronics department. Fig.1 presents the designed readout scheme. The basic element of this readout system is a 48-channel ASF48et board (Fig.2) designed specially for this experiment. At present, one such board is constructed and is under tests.

Selection of true ep collisions

The trigger is a recoil signal ($T_R \geq 0.3$ MeV) detected in TPC at time t_R . The maximal drift time in TPC is 100 μs . Therefore, any beam electron which appeared in TPC in the time interval $t_R - 100 \mu\text{s} \leq t \leq t_R$ should be considered as a candidate for the recoil parent particle. The electron beam intensity is $2 \cdot 10^6$ electrons per second. That means that the **average number of the ep candidates at this stage is 200**.

The selection of the true ep scattering event is needed for finding the correct Z- coordinate of the ep collision vertex. This selection can be done off-line in the following steps of the analysis of the registered data.

Selection step1. Beam detector&Forward Tracker coincidence.

Our MC calculations show that each electron entering TPC can create charge particles in the FT acceptance (from 20 mrad to 450 mrad) with a probability 2.3% while the beam particles are concentrated in the central dead zone of the FT. That means that

the BD@FT coincidence (within 5 ns resolution time of FT) will reduce the number of the ep candidates by a factor of 40. Still **5 candidates** in average will remain.

Selection step 2. Tracing back of the electron trajectory.

The remaining candidates with arrival times t_i (determined by BD) correspond to different coordinates of the ep vertex: $Z_i = W(t_i - t_R)$ where W is the drift velocity. Tracing back the electron trajectory determined by the FT1 and FT2 planes, one can determine the Z_{back} coordinate and compare it with Z_i . The precision of Z_{back} determination depends on the angle θ_e of the electron trajectory. It is about 5 mm (sigma) for $\theta_e = 25$ deg. and ~ 2 cm (sigma) for 5 deg. Correspondingly, the rejection power of this method varies from factor 20 down to factor 5 (the difference $Z_{back} - Z_i$ on a level 4 sigma). So one can expect the reduction of the false candidates at least by a factor of 5. **What remains is one false candidate in average per one true ep event.**

Selection step 3. Correlation $\theta_e - T_R$.

The $\theta_e - T_R$ correlation provides a powerful background rejection. Together with the previous selection steps, **this allows to select the true ep events on a very high confidence level with $\sim 100\%$ detection efficiency.**

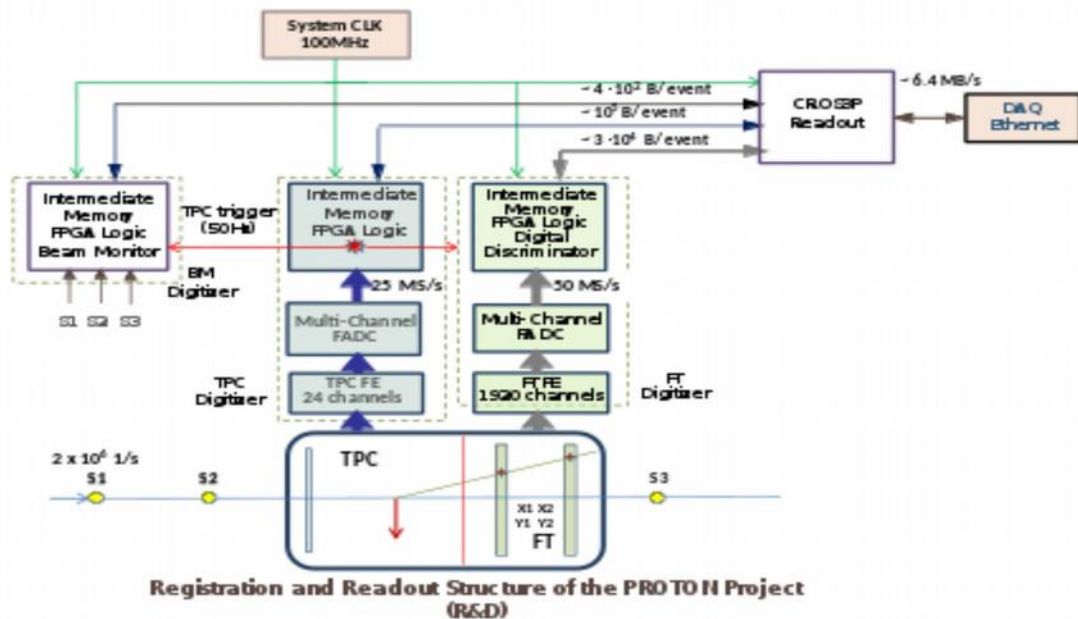


Fig.1 The readout scheme for TPC@ FT detector

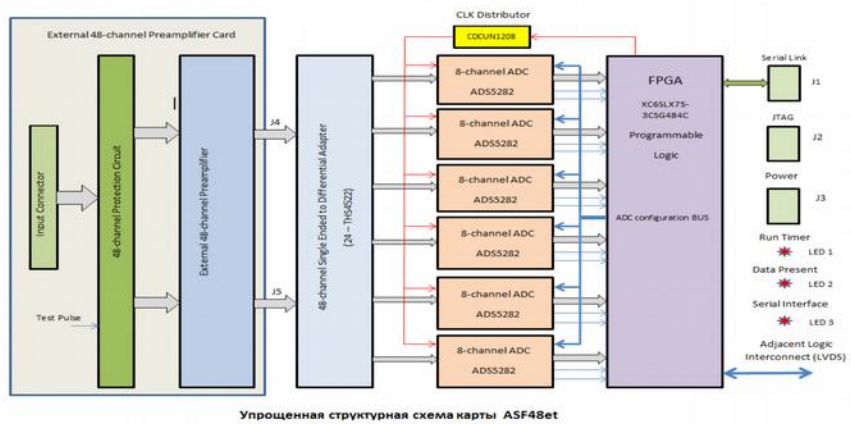


Fig.2 Simplified structure scheme of the ASF48et board

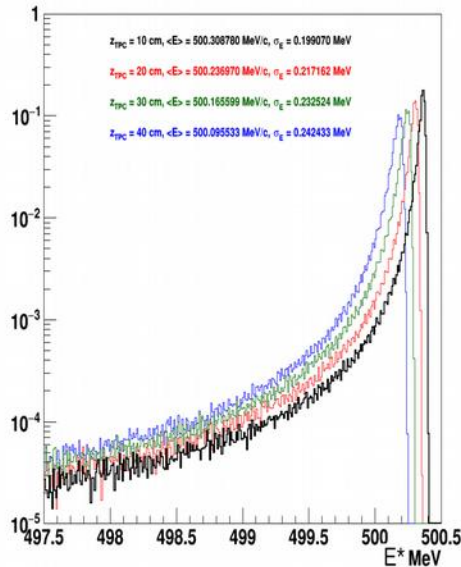
Annex 5

Calibration of the recoil proton energy scale

The calibration of the TPC t-scale foreseen in this experiment relates the observed signals from TPC (S_{TPC}) with the absolute t-values determined from the measured θ_e distributions. The calibration will be done using the whole set of collected real experimental data. For that, we select a bin ΔS_{TPC} in the 2D plot $S_{\text{TPC}} - \theta_e$ and look at the corresponding θ_e distribution. This will be a peak at θ_{eM} with a tail to larger angles due to the energy losses of the electron before the ep collision. However, the maximum of the spectrum at θ_{eM} (with corrections for the energy losses before the ep-collision) should correspond to the undisturbed incident beam energy ε_e thus allowing to determine the t-value corresponding to the selected S_{TPC} bin.

This procedure is illustrated below by MC simulation of the ep elastic scattering events at 500 MeV/c beam momentum. The beam electrons entered TPC through a 5mm Be window. Fig.1 shows the total energy of the electrons in the ep collision point at different Z_{TPC} .

Electron energy E^* in the collision point



32

Fig. 1. Total energy E^* of the electrons in the collision point after traversing the TPC window (0.5mm Be) and hydrogen gas (20 bar pressure). The initial electron momentum 500 MeV/c.

One can see in these distributions well defined peaks shifted from the initial electron energy by up to 400 keV at the TPC end ($Z=400$ mm).

Now we can fix the energy of the recoil proton and look at the angular distribution of the scattered electrons. Fig.2 shows an example of such distribution for $T_R = 10$ MeV and $z = 10$ mm. Shown are two options of measuring the scattering angle.

In the first option, the angle is determined by the known vertex in TPC and the X1/Y1 coordinates measured by the first CSC station. In the second option, the angle is determined independently from TPC using X1/Y1 and X2/Y2 coordinates from the CSC stations. Both options give identical result $\theta_e = 277.517$ mrad instead of expected $\theta_e = 277.358$ mrad.

If one calculate the transfer momentum with this angle without correction for the electron energy loss before the collision, in this case the ratio of thus determined transfer momentum to the real transfer momentum will be $1 + 1.2 \times 10^{-3}$.

However, one can apply this correction calculated by MC. In this case the ratio becomes equal to $1 + 3.8 \times 10^{-4}$. This result is already acceptable for the t-scale calibration.

One can improve the agreement even further by taking into account the asymmetry in angular distribution of the scattered electrons caused by radiation losses. As it is shown in Fig.3, the radiation tail slightly shifts the peak value to larger angles. If we take into account this shift, then the ratio of the transfer momentum determined in this procedure to the real transfer momentum will be $1 + 0.8 \times 10^{-4}$.

One should stress again that such calibration will be done directly in the course of data analysis using the whole set of collected experimental data. Therefore, any small changes in the experiment in the parameters determining the measured recoil energy (such as signal shaping) will be automatically taken into account.

Conclusion

With the described method, the t-scale (T_R scale) calibration can be done with 0.02% relative precision. The cited in the proposal 0.04% precision takes also into account the systematic errors in the linear scales in the cathode planes in CSCs.

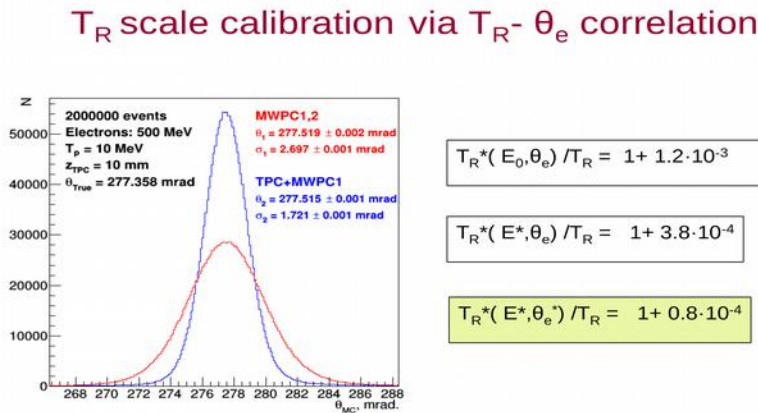


Fig.2. Angular distribution of electrons scattered in TPC at $z=10$ mm with selected transfer momentum $T_R = 10$ MeV. MC simulation.

θ_e^* corrected for the radiation tail

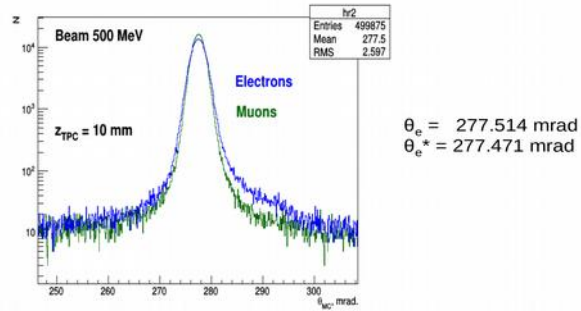


Fig.3. Comparison of angular distributions of scattered electrons and muons. The tail in the electron spectrum results in a 0.043 mrad shift in the average angle determined in the selected θ - region.